Eur Biophys J (2006) 36:35–43
DOI 10.1007/s00249-006-0088-0

ARTICLE

Homology modeling of tubulin: influence predictions for microtubule's biophysical properties

Eric J. Carpenter · J. Torin Huzil · Richard F. Ludueña · Jack A. Tuszynski

Received: 5 April 2006 / Revised: 17 July 2006 / Accepted: 27 July 2006 / Published online: 29 August 2006

Abstract Using comparative modeling, we have generated structural models of 475 α and β tubulins. Using these models, we observed a global, structural similarity between the tubulin isotypes. However, a number of subtle differences in the isotypes physical properties, including net electric charges, solvent accessible surface areas, and electric dipole moments were also apparent. In order to examine the roles that these properties may play in microtubule (MT) assembly and stability, we have created a model to evaluate the dipole–dipole interaction energies of varying MT lattice conformations, using human tubulin isotypes as particularly important examples. We conclude that the dipole moments of each tubulin isotype may influence their functional characteristics within the cell, resulting in differences for MT assembly kinetics and stability.

Keywords Tubulin · Isotype · Comparative/homology modeling · Microtubule · Dipole

E. J. Carpenter · J. T. Huzil · J. A. Tuszynski (✉)
Department of Oncology, Division of Experimental Oncology, University of Alberta, Cross Cancer Institute, Edmonton, AB, Canada T6G 1Z2
e-mail: jtus@phys.ualberta.ca

J. A. Tuszynski
Department of Physics, University of Alberta, Edmonton, AB, Canada T6G 2G7

R. F. Ludueña
Department of Biochemistry, University of Texas Health Science Center at San Antonio, San Antonio, TX 78229-3900, USA

Introduction

Microtubules (MTs) are hollow cylinders constructed from linear chains, or protofilaments, of repeating subunits of α and β tubulin. MTs are involved in many cellular processes within eukaryotic organisms, including maintenance of cell morphology and active transport of proteins and organelles throughout the cytoplasm (Pichichero and Avers 1973; Hyams and Stebbings 1979). MTs go through periods of assembly and disassembly, a property known as dynamic instability (Mitchison and Kirschner 1984). Dynamic instability has been extensively investigated and is critical during mitosis when a delicate equilibria of forces are necessary for proper chromosome alignment prior to segregation (Margolis and Wilson 1981; Horio and Hotani 1986; Kirschner and Schulze 1986; Melki et al. 1989; Walker et al. 1991; Mandelkow and Mandelkow 1992). The correct assembly of MTs into the mitotic spindle is essential, as it likely provides the mechanical force for mitotic chromosome segregation (Westermann et al. 2006). The failure of this assembly process generally results in mitotic arrest and for this reason, several chemotherapeutic agents disrupt normal cell division by targeting MTs (Jordan and Wilson 2004).

Most eukaryotic organisms have multiple genes which encode distinct isoforms or isotypes of α and β tubulin. In humans, several isotypes have been identified and characterized (Lu and Luduena 1994; Roach et al. 1998; Luduena 1998). In addition to α and β tubulin, three other tubulin homologues are required for efficient MT assembly in vivo. The first, γ tubulin, is not essential for assembly, yet is found at MT-organizing centers and is thought to aid in initial MT nucleation (Oakley et al. 1990). Two other

homologues, δ and ε tubulin, have uncertain roles in MT assembly, although models have been proposed that describe their possible involvement in MT self-assembly (Inclan and Nogales 2001). At the molecular level, the roles and interactions of tubulin are complex and differ between isotypes. For instance, MT dynamics appears to change significantly with β tubulin isotype composition (Panda et al. 1994). This result implies that if MT assembly/disassembly equilibria are disrupted, cells might respond by producing an appropriate isotype mix to restore normal balance. While the presence of numerous tubulin isotypes, whose differences are often highly conserved in evolution (Ludueña 1998), suggests that they may play specific roles in MT function, there are no precise models to describe differences between them.

A major advance in our understanding of MT structure and function was the solution of tubulin's three-dimensional crystallographic structure (Nogales et al. 1998). Several crystallographic structures of tubulin are now available from the RCSB Protein Data Bank (PDB) and we refer to these structures by their PDB ID (Berman et al. 2000). The first approach to obtain tubulin crystals was taxane-stabilized bovine-brain tubulin (mixed isotypes) in flat Zn^{2+} induced sheets, producing protofilament-like end-to-end α/β dimer repeats. The earliest structure, 1TUB, utilized a drug known as docetaxel to stabilize protofilaments for crystallography (Nogales et al. 1998). Due to difficulties in fitting to the electron density, this structure contains several misalignments and density omissions and was superceded by 1JFF, which utilized paclitaxel, a drug similar to docetaxel, to stabilize the protofilaments (Lowe et al. 2001). Similarly, the structure 1TVK utilized the drug epothilone A, which binds at the paclitaxel/docetazxel binding site (Nettles et al. 2004). One final structure from this group, 1IA0 contains direct copies of the 1TUB monomers which were docked with the monomeric kinesin motor KIF1A (Kikkawa et al. 2001). A second approach to producing tubulin crystals utilizes the stathmin-like domain RB3-SLD, which complexes a pair of α/β dimer repeats. The earliest of these, 1FFX, utilized molecular replacement from the 1TUB data (Gigant et al. 2000). Most recently two higher resolution structures, 1SA0 and 1SA1, were co-crystallized with colchicine and podophyllotoxin, respectively (Ravelli et al. 2004), while both colchicine and vinblastine are included in 1Z2B (Gigant et al. 2005). Other, non-eukaryotic or tubulin-like structures also exist. The structures, 1Z5V and 1Z5W, are of human γ tubulin crystals (Aldaz et al. 2005). Related prokaryotic structures include 2BTO and 2BTQ products of *Prosthectobacter dejongeii* genes BtubA and BtubB (Schlieper et al. 2005). Additionally, several structures of the prokaryotic tubulin homolog FtsZ are also available.

The availability of high quality structural data for tubulin has enabled us to create comparative models of all currently known α and β tubulin isotypes. Comparative modeling uses known protein structures as templates to produce 3D structural models of a target protein with a known, related amino acid sequence. By assuming that parts of the target and templates with similar sequences have similar 3D structures, portions of the template structures may be copied and amino acids substituted, inserted, or deleted to produce models. Any part of the target not obtained from the template structure must be constructed via de novo methods. Finally, the resulting model must then be optimized to a protein-like geometry. This technique has been verified for a small number of homologous protein families and can yield accurate results for template/target pairs with strong sequence identity (Chothia and Lesk 1986).

From such comparative models, we have calculated the energy associated with MT lattice dipole–dipole interactions for all the human tubulin isotypes. Schoutens (2005) estimated that MT dipole–dipole interactions destabilize the MT structure by 50–60% of the elastic energy of the underlying lattice. The strength of these interactions is roughly proportional to the squares of the dipole moments; increased tubulin dipole moments should therefore make MTs less stable. From our estimates we hope to understand how tubulin isotype sequences may affect both MT assembly and stability through basic electrostatic properties of protein.

Materials and methods

Tubulin sequences

Tubulin sequences were obtained from the Uniprot Knowledgebase, consisting of Swiss-Prot release 42.1 and TrEMBL release 25.12 (15 March 2004) (Boeckmann et al. 2003). The entire database was downloaded and sequences annotated with the term ''tubulin'', were extracted, producing an initial set of 2,294 entries. This initial set was then filtered to remove entries labeled as fragmentary, leaving only 652 complete tubulin sequences. These sequences were then aligned and using cluster analysis assembled into a guide tree, or dendrogram using default parameters within Clustal W (version 1.82) (Higgins and Sharp 1988). This step identified sequences that are not tubulin, but unrelated

proteins with tubulin in their name (e.g. tubulin tyrosine ligase or tubulin-folding cofactor D). Since these nontubulin sequences differ significantly from the tubulins, they clustered separately in the dendrogram, providing a clear delineation between 557 ''tubulin-like'' and 95 nontubulin sequences. A second dendrogram guide tree was then produced using only the ''tubulin-like'' sequences resulting in three major branches, one of 190 α tubulin sequences, one of 285 β tubulin sequences, and the third of 82 tubulin sequences that were neither α nor β tubulin.

Template selection

As we were constructing models of eukaryotic α and β tubulins, we rejected γ tubulin and bacterial proteins as structural templates. We chose to use only monomers from the 1JFF and 1SA0 structures as these are high-resolution representatives of the two crystallographic approaches. We also reasoned that all three tubulin dimers within these structures have distinct environments and would produce variation in the models. In the 1SA0 structure, the colchicine molecule is at opposite ends of the two dimers and each dimer has a different interaction with the stathmin-like domain, while the 1JFF dimer is in a different crystal packing. Thus, for α tubulins we used the 1JFF A chain and the 1SA0 A and C chains, while for β tubulins we used the 1JFF B chain and the 1SA0 C and D chains.

Modeling

To build the models, we used Modeller (version 6v2) (Sanchez and Sali 2000). While Modeller provides many options for model refinement and fine-tuning, default parameters and settings were deemed sufficient for generating the models presented here. (See Table 1 for a sample script building sequence P05218 on the 1JFF β monomer.) For each tubulin sequence, three models were built, each using a different one of the three templates (Table 1). To check the correctness of each of the models, some were tested with PROCHECK and WHAT_CHECK (Laskowski et al. 1993; Hooft et al. 1996). Since the results of these programs require human inspection, only a small subset of models was tested in this way. These results suggested to us that the isotype models are likely of similar quality to the input template structures. As a final step, models were re-positioned onto the coordinates of the templates used to create them by RMSD (root-mean-square deviation) fitting over corresponding alpha-carbons.

Generation of human isotype models

Among the 190 α and 285 β tubulin sequences are 22 human sequences. Two are quite different in length from the templates, one short (Q8WU19), and one long (Q8WUL7). The other 20 were used to examine the stability of the modeling technique and accuracy of the models by producing 100 models of each target. As Modeller uses pseudo-random noise in model construction, each differs slightly, providing a sample of 100 Modeller output conformations for these human sequences.

Calculations of the surface areas, charges, and dipole moments

After models were built, surface areas, total charges, and dipole moments were estimated using analysis tools in Gromacs v. 3.3 (Lindahl et al. 2001). Models were converted using pdb2gmx with the GROMOS96 43a1 force field (van Gunsteren 1996), providing atomic charges, sizes, and some hydrogen atom

Table 1 Sample MODELLER routine

```
# comparative modelling by the MODELLER TOP routine MODEL
SET KNOWNS = '1JFFB'                    # code of the templates
INCLUDE                                 # load Modeller defaults from __defs.top
READ_TOPOLOGY FILE = '$(LIB)/top_heav.lib'
# read template sequence
READ_ALIGNMENT FILE = 'structure.ali', ALIGN_CODES = KNOWNS
# add sequence to be modeled, remembering how many templates are already aligned
SET ADD_SEQUENCE = ON, ALIGN_BLOCK = NUMB_OF_SEQUENCES
READ_ALIGNMENT FILE = 'tubulins.ali', ALIGN_CODES = ALIGN_CODES 'P05218'
# align sequence to template
ALIGN2D
# save alignment – read by routine MODEL
WRITE_ALIGNMENT FILE = 'P05218.ali'
# do model construction
CALL ROUTINE = 'model', ALNFILE = 'P05218.ali', SEQUENCE = 'P05218'
STOP
```

locations. As a side effect, the net charge of the sequence is reported, assuming charges of $+1e$ for lysine and arginine, $-1e$ for aspartic and glutamic acids, and no charge for other residues. Using g_sas, Connolly solvent accessible surfaces (SAS) were then calculated (Connolly 1983). Next, editconf was used to shift the co-ordinate origin to the model's geometric center, which is expected to be a good approximation of the monomer's center-of-mass. Dipole moments were then calculated using g_dipoles. These dipole components were then converted to a cylindrical coordinate system based on MT geometry. Each 1SA0 monomer was α-carbon RMSD fit onto the corresponding 1JFF monomer, these transformations taken as conversions between the 1SA0-based co-ordinate space and a 1JFF-based one; 1JFF co-ordinates were converted to the MT-based one by 63° rotation about the protofilament axis, a value chosen with data presented by Li et al. (2002). Each dipole moment was transformed identically to its model's template.

Calculations of the microtubule dipole–dipole interaction energies

The same MT geometry based cylindrical coordinate system, as described above, was used for dipole interaction energy estimates. We defined a direction away from the central cylindrical axis as radial, one parallel to the central axis as longitudinal, and one perpendicular to both of these (around the surface of a cylinder) as tangential. Following the description by Li et al. (2002), we position dipoles at a radius of 112 Å, in 13 parallel protofilament-like rows, at the 13 angular multiples of (360/13)°. Along these rows, dipole values were placed every 81.2 Å

The interaction energy between two dipoles $\vec{p}_1$ and $\vec{p}_2$ separated by $\vec{r}$ is given by:

$$U = \frac{1}{4\pi\varepsilon\varepsilon_0}\left(\frac{\vec{p}_1\cdot\vec{p}_2}{r^3} - 3\frac{(\vec{p}_1\cdot\vec{r})(\vec{p}_2\cdot\vec{r})}{r^5}\right). \quad (1)$$

Each dipole is described as

$$\vec{p} = (p_r, p_\theta, p_z),$$

having a radial, tangential, and longitudinal component. The interaction energy of two dipoles of known positions can then be rewritten:

$$\begin{aligned} 4\pi\varepsilon\varepsilon_0 U = {} & c_1 p_{r1} p_{r2} + c_2 p_{r1} p_{\theta 2} + c_3 p_{r1} p_{z2} \\ & + c_4 p_{\theta 1} p_{r2} + c_5 p_{\theta 1} p_{\theta 2} + c_6 p_{\theta 1} p_{z2}, \\ & + c_7 p_{z1} p_{r2} + c_8 p_{z1} p_{\theta 2} + c_9 p_{z1} p_{z2}, \end{aligned} \quad (2)$$

where the nine c_i are known geometry-dependent constants dependent on $\vec{r}$ and the rotation of coordinate system components between the two dipoles.

To calculate the interaction energy between a reference dipole and those in an adjacent protofilament, as the adjacent protofilament is displaced along its length, we take several dipoles from the adjacent protofilament near the reference and evaluate the c_i of (2) between adjacent dipoles and the reference. Then with all the adjacent dipoles identical, and $4\pi\epsilon\epsilon_0$ uniform, the p are common factors for all interaction pairs, so each of the nine c_i terms can be separately summed over all pairs to obtain a total dipole–dipole energy of the same form as (2), with a new set of c_i.

We evaluated summations over adjacent sections of length $2l + 1$, expecting that as we summed longer sections we would approach a limit, more separated dipole pairs having weaker interactions. We placed the reference dipole at $z = 0$ Å and the adjacent dipoles at $z = (81.2\text{ Å})(i + d)$ where integer $i \in [-l,+l]$, and the displacement, d, varied from 0 to 1. At $d = 0$, we found that a limit is rapidly approached in our calculations, with little difference in the summed c_i for several $l \geq 10$, and those of $l = 10{,}000$.

For $l = 1{,}500$ and d = 0.00, 0.01, 0.02,...,1.00 we calculated the summed values of the nine coefficients c_i and observed near sinusoidal variation with displacement (Fig. 1). Fits to the three lowest frequency Fourier components,

$$c_i(d) = A_i + \sum_{k=1}^{3} B_{ki}\cos kd + C_{ki}\sin kd,$$

give coefficients where either the sine or the cosine series coefficients are large (more than one part in 10^6) relative to those of the other series. In this significant series the second-order terms are all less than 5% of the first-order terms, and the third-order terms less

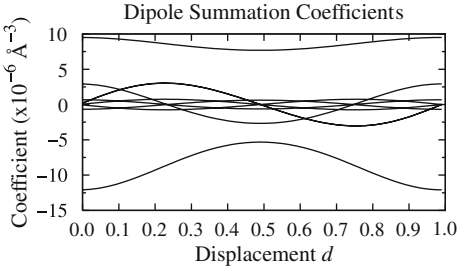

Fig. 1 The nine coefficients c_i as functions of the displacement, d for the case of an adjacent protofilament. Note the high level of symmetry, and that two of the nine curves are identical and superimposed in the plot

than 3% of the second-order terms. In only two of the nine cases are the constant terms significantly nonzero. Thus, we take only the first order and constant terms and obtain the approximations $c_i(d) \approx A_i + B_i \cos d$ or $c_i(d) \approx C_i \sin d$. We note that this approximation implies sinusoidal variation with displacement to the energy in (2).

This calculation can be easily extended to the dipole interactions between a reference dimer and an adjacent protofilament when each monomer has its own dipole moment. Treating the α and β contributions in the two filaments separately gives four cases. In the first, we can place all the α dipoles at the locations discussed above and obtain the same result. The case of the row of β dipoles midway between adjacent α row interacting with the reference α dipole has the same form but an additional one-half displacement is included. Similarly, a reference β dipole may be placed at $z = 40.6$ Å, the same as subtracting one-half from the displacements when interacting with the row of α dipoles. In the β–β interactions case, the two additional displacements cancel out. By summing the contributions of the four cases, a single sum is again obtained. For simplicity, we use only one α and one β monomer in both the adjacent and reference positions. Then by symmetry, many coefficients cancel and the result may be rewritten as

$$4\pi\varepsilon\varepsilon_0 U = F + G\cos d \tag{3}$$

where both F and G have the form

$$\begin{aligned} &e_1(p_{r\alpha}^2 + p_{r\beta}^2) + e_2(p_{\theta\alpha}^2 + p_{\theta\beta}^2) + e_3(p_{z\alpha}^2 + p_{z\beta}^2) \\ &\quad + e_4(p_{r\alpha}p_{r\beta}) + e_5(p_{\theta\alpha}p_{\theta\beta}) + e_6(p_{z\alpha}p_{z\beta}) \end{aligned} \tag{4}$$

for particular values of the geometric constant coefficients e_i.

Results and discussion

Comparative modeling is a theoretical method with predictive power limited by the degree of similarity between target and template structures and input template quality. Quality is further limited by the choice of refinement approximations following model construction. Further constraints on predictive power arise from failures to include environmental factors, such as ligands, ranging from ions to protein complexes, and chemical modifications such as post-translational modification, both of which are relevant in the case of tubulin.

Tubulin sequences

Our set of α and β tubulin sequences includes animal, plant, fungal, and protist tubulins. We believe that this set is likely large enough to well sample the diversity present within the tubulin family. In general, the tubulin sequences modeled were similar to those of the templates. However, some of the tubulin sequences vary greatly in length from the template sequences. It seems likely that some of these sequences may not assemble into MTs, e.g. a γ tubulin sequence. Such cases would be less well modeled using this technique than other sequences. Except for the two human sequences omitted during the human repeat calculations, such possible problems were ignored and all sequences were treated identically.

It should be noted that the assignments generated by the initial clustering did not always agree with the database labels. Alignments and scoring were performed without knowledge of each isotypes cellular function, close similarity between the isotypes occasionally produced ambiguous results. For instance, the Uniprot Knowledgebase sequence Q94EN1 is described as ''Pi-tubulin'' in the database, but clustered within the α tubulin set using the procedure described above.

Template selection

All of the available tubulin structures would likely provide good templates for modeling. All structures of crystallized α and β tubulin are similar, being nearly indistinguishable at 6 Å, even with only 40% amino acid identity between them (Li et al. 2002). Since sequences within the α and β tubulin groups are more similar to sequences within the same group than with those of the other group, it is reasonable to expect that any given sequence likely has a structure very similar to that of other members of its group. An example is the 1TUB and 1JFF structures which are of a porcine sequence, but fit to structural data from inhomogeneous bovine samples. Accordingly, either crystallographic structure can be used as a template to produce models with some confidence. However, each of these template structures contains missing or weakly defined residues. Trivially, neither template contains the initial methionine residue. Additionally, one α tubulin loop is incomplete with residues Q35–L60 missing from the A chain in 1JFF and residues P37–D46 and S38–D46 missing from the A and C chains of 1SA0, respectively. Both of the 1SA0 β monomers, chains B and D lack residues R278–A285 and several side chains within these structures are also truncated. Further, all

template structures lack a 20–30 residue region, commonly referred to as the C-terminal tail (approximately residue 440 to the C-terminus); this region is believed to be highly flexible. Within these missing regions the model is being created with few constraints and less confidence should therefore be placed in the reality of the results.

Comparison of the tubulin models shows that regions found within the templates have well-defined structures, and those without templates are more disordered. The region missing from the 1JFF α tubulin template (Q35–L60) produces a large unstructured loop away from the core of the monomer in many models. The large variability of this region within the human repeats led us to reject the 1JFF α tubulin derived models from further consideration. In the 1SA0-based models, due to the resolved structure of more of the template, this region has a more compact structure, although it is more variable than most other regions in the models. In all the models, loops corresponding to residues 360–371 and 275–286 are also of high variability, owing to unresolved structures in the templates. Such variations within the structure of tubulin could have an effect on dimer–dimer interactions, which may translate into significant changes in assembly/disassembly rates for MTs. These differences are fairly well studied experimentally (Panda et al. 1994) but poorly understood theoretically. It should be noted that the generated C-terminal regions are too flexible and variable for models to represent, at best, more than one of many possible conformations. To what extent the variation in the models is experimental artifact, and to what extent real variation in the tubulin structures is unknown.

Estimation of physical properties

It is possible to estimate various physical characteristics from these models. These properties can then be considered for possible effects of these on tubulin dimer–dimer interactions, and thus MT assembly and stability. One contribution to the interactions between tubulin dimers is the electrostatics of each tubulin monomer, in particular, net charges and dipole moments. The net charge or monopole is perhaps the simplest approximation to the complicated electrostatic field around a protein. Slightly more complex is the electrostatic dipole moment, which has opposing positive and negative directions along a central axis, and is radially symmetric about this axis. Like the monopole, the dipole is an average over a real system and is generally inadequate for representing the complex field near a protein, and is also subject to attenuation by solvent mediated effects, but having both a position and an orientation, a dipole may give more complex interactions. With charges at points in space, we can calculate a dipole moment about a chosen coordinate origin. If a system has zero net charge, this dipole moment is independent of the choice of origin, but is otherwise dependent upon the origin. For protein dipole calculations, the center-of-mass is commonly used.

Solvent accessible surface area

For each tubulin model, we estimated the solvent accessible surface areas and show that they are largely the same for α and β tubulins with mean areas of approximately 220 nm^2, and standard deviations of 10 and 30 nm^2, respectively. This difference in variance is visible where surface areas for α and β tubulins are compared with their estimated dipole moments (Fig. 2). Little correlation between these two properties is evident from these scatter plots. However, there does appear to be an observable difference within the mean dipole between the alpha and beta tubulin.

Electrostatics

Tubulin sequences generally contain more acidic than basic residues and accordingly we report negative electrostatic charges. In an overly simplistic analysis we could expect that these negative charges would repel, thereby preventing MT formation. However, at short ranges charge is partially screened and some close charge pairs can dominate the electrostatic interaction

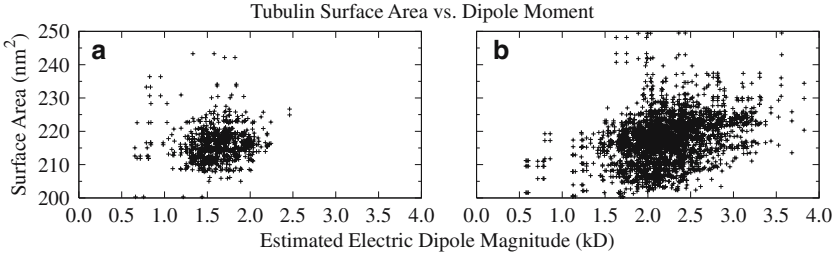

Fig. 2 Comparison between tubulin isotype models solvent accessible surface areas and estimated dipole moment magnitudes. Panel **a** illustrates correlation within α tubulin models. Panel **b** illustrates correlation within β tubulin models

over more distant pairs. The extreme of this occurs between monomers, where contacting regions have interactions strong enough to form a stable bond.

The α tubulins are estimated to have dipole magnitudes about their centers in the range 1,000–2,000 D, while β tubulin magnitudes are generally higher, in the range 2,000–3,000 D (Fig. 3). The β tubulins are, on average, more highly charged with an approximate mean of –24*e*, compared with –22*e* for the α tubulins. The β tubulins also have a slightly broader net charge distribution than α tubulins (standard deviation of 3.0*e* versus 2.6*e*). There appears to be little if any correlation, in the scatter plots, between the dipole moment and the net charge as might be expected since polynomial expansions coefficients such as the electrostatic potential generally have no dependence on one another (Fig. 4).

In this work we give specific values for tubulin charges and dipole moments. It is important to recognize that these values only consider the protein and not effects due to the surrounding solution. A significant solvation effect is on mean protonation state; net tubulin charge becomes more positive as pH decreases. In particular, near pH 5, tubulin is electrically neutral (pI from SWISS-2DPAGE, see Hoogland et al. 2004). However, our electrostatic numbers are derived with a charge model (Gromos96 43a1) with a specific charge for each atom, appropriate near pH 7. Another solvation effect is counter-ion cancellation of the electrostatic field about a charged object. Charge effects only occur when there is some separation of this screening charge and the charge. Trivially, objects in close proximity will exclude some or all of the screen. More generally, this separation will depend on the solution composition. Since the extent of screening will depend on the circumstance we report values for unscreened systems, and as a further simplification use uniform dielectric constants.

Comparing our calculated values to experimentally based values reveals the possible magnitude of these solvent effects. For instance, experiments orienting or dragging MTs with external electric fields have reported per dimer charges equivalent to –0.9*e* and –0.2*e* (Minoura and Muto 2006; Stracke et al. 2002). These results may also be interpreted as a measure of the screening charge pulled away from the tubulin. In a different example, the addition of tubulin to a solution is reported to affect the high-frequency dielectric constant by 0.0050 mL/mg (Schuessler et al. 2003). Using this value in the dilute limit Oncley formula gives a tubulin dipole moment of 78 D for a dimer at 300 K. While our values do not compare well with these numbers, but it must be emphasized that we did not expect them to be considered absolute and are only valid within the results presented here.

Human isotypes

The 100 models of the human tubulin sequences allow the reproducibility of results for an isotype sequence to be assessed. In particular, the dipole moment estimates have roughly a 300 D standard deviation. These values suggest that much of the observed variation between sequences may be attributed to model variability and not intrinsic differences among the sequences. For one of the 55 sequence-template pairs in this repeat set, Modeller stopped prematurely with an error, so 64 of the 5,500 repeat models were not built.

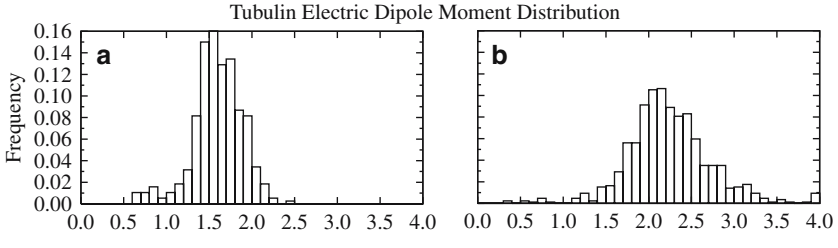

Fig. 3 Distribution of the estimated dipole moment magnitudes for α tubulin (**a**) and β tubulin (**b**)

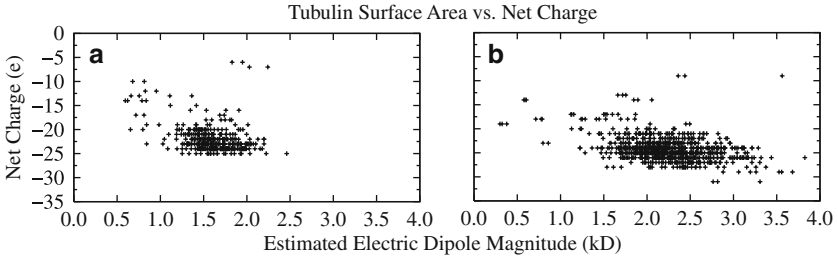

Fig. 4 Comparison between the dipole moments and net charges for α tubulin (**a**) and β tubulin (**b**)

Human microtubule dipole interaction energies

We considered all the α/β pairings of models from our set of replicate human runs, and evaluated all of the dipole moments with (3). We noted G, the sinusoidal magnitude, is typically small compared to F, the offset term, and so we ignored the sinusoidal term. The results show a great deal of similarity, with the five α monomers being largely indistinguishable, as are many of the β monomers; only the Q99867 sequence is significantly different. The distribution of interaction energies for $\epsilon\epsilon_0 = 1$ of each human β tubulin sequence is shown in Fig. 5a. A similar calculation can be done within a single protofilament by replacing a dimer in the ''adjacent'' protofilament with the reference dimer. Displacement makes no sense in this case, avoiding the sinusoidal term (Fig. 5b). Again, only Q99867 stands out as significantly different in this regard.

Summary and conclusions

We have used comparative modeling as a computational tool to generate structural models of 475 α and β tubulin sequences. We note a structural similarity across tubulin isotypes, along with some subtle differences in physical properties, including net electric charges, solvent accessible surface areas, and electric dipole moments. In order to examine the roles these properties may play in MT assembly and stability, we evaluated dipole–dipole interaction energies of MT lattice conformations with various human tubulin isotypes. In this case, we already know that isotype composition affects MT assembly kinetics (Panda et al. 1994). We therefore expected that properties, such as the dipole moment, may influence the functional behavior of tubulin monomers and dimers within the cell, resulting in differences for MT stability and assembly kinetics. It was demonstrated that electrostatics contributes to the energy of relative longitudinal offsets between two protofilaments, helping to shape the energy minima corresponding to the two MT lattice types, especially the A-lattice (Sept et al. 2003).

Further, besides its involvement in MT stability, the dipole moment of tubulin may play a role in other processes involving tubulin, for example, docking of molecules such as kinesin or MT associated proteins to tubulin and in creating the proper steric configuration of a tubulin dimer as it approaches an MT for binding. Interestingly, in an MT, dimers have near parallel dipole moments relative to their nearest neighbors, suggesting energy minimization takes place during MT assembly. However, when all dimer–dimer interactions in a MT are summed, the total is a positive energy leading to MT destabilization. Hence the greater the magnitude of the individual dipole moments (assuming all are identical), the less stable the MT since these interactions will be repulsive, pushing dimers apart. The strength of these interactions is proportional to the squares of the dipole moments; MTs made up of tubulin with larger dipole moments should be more prone to disassembly than those composed of lower dipole moment tubulins. For cells expressing more than one isotype, one can conceive MT dynamics regulated by altering relative amounts of isotypes. However, these effects are moderated by local interactions with more complicated electrostatic fields than the above simplified assembly of dipoles; for details see Baker et al. (2001). Nonetheless, it is possible that the differing kinetic properties of different isotypes are linked to the electrostatic differences.

From the discussion of experimental determinations of electrostatic properties of tubulin and MTs it is clear that the experiment and its precise conditions can ultimately affect the outcome of any measurement. Hence, we require more accurate and systematic analyses under a range of conditions such as pH, ionic concentrations, tubulin concentration, and temperature values. It is, however, clear that electrostatics, and in particular the dipole moment, plays an important role in the interactions of tubulin with itself, with other proteins, molecules, and ions.

Acknowledgments This work has been supported by grants from NSERC (Canada), MITACS and grants to R. F. L. from the Welch Foundation (AQ-0726), US Department of Defense BCRP (W81XWH-05-1-0238) and the PCRP (W81XWH-04-1-0231).

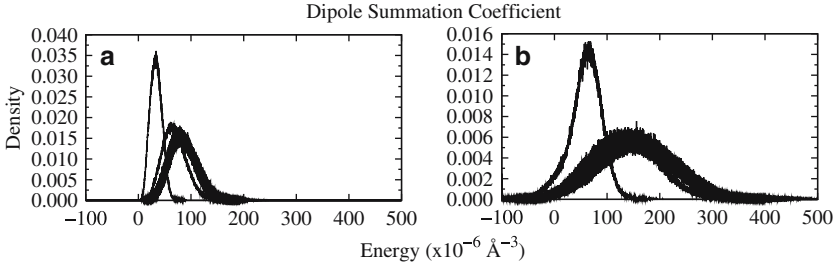

Fig. 5 The per dimer interaction energies within a microtubule for all human tubulin isotypes. Panel **a** illustrates results obtained for adjacent protofilaments within a MT structure. Panel **b** illustrates results for a single protofilament using a reference dimmer only

This work was also supported through a grant from the Canadian Prostate Cancer Research Initiative (016501). Additional support has come from grant P30-CA54174 from the National Institutes of Health to the San Antonio Cancer Institute. Financial support for this project from Technology Innovations, LLC of Rochester, NY, is gratefully acknowledged.

References

Aldaz H et al (2005) Insights into microtubule nucleation from the crystal structure of human gamma-tubulin. Nature 435:523–527

Baker N et al (2001) Electrostatics of nanosystems: application to microtubules and the ribosome. Proc Natl Acad Sci USA 98:10037–10041

Berman HM et al (2000) The protein data bank. Nucleic Acids Res 28:235–242

Boeckmann B et al (2003) The SWISS-PROT protein knowledgebase and its supplement TrEMBL in 2003. Nucleic Acids Res 31:365–370

Chothia C, Lesk A (1986) The relation between the divergence of sequence and structure in proteins. EMBO J 5:823–826

Connolly M (1983) Solvent-accessible surfaces of proteins and nucleic acids. Science 221:709–713

Gigant B et al (2000) The 4 A X-ray structure of a tubulin:stathmin-like domain complex. Cell 102:809–816

Gigant B et al (2005) Structural basis for the regulation of tubulin by vinblastine. Nature 435:519–522

Higgins D, Sharp P (1988) CLUSTAL: a package for performing multiple sequence alignment on a microcomputer. Gene 73:237–244

Hooft RW et al (1996) Errors in protein structures. Nature 381:272

Hoogland C et al (2004) SWISS-2DPAGE, ten years later. Proteomics 4:2352–2356

Horio T, Hotani H (1986) Visualization of the dynamic instability of individual microtubules by dark-field microscopy. Nature 321:605–607

Hyams JS, Stebbings H (1979) The mechanism of microtubule associated cytoplasmic transport. Isolation and preliminary characterisation of a microtubule transport system. Cell Tissue Res 196:103–116

Inclan Y, Nogales E (2001) Structural models for the self-assembly and microtubule interactions of gamma-, delta- and epsilon-tubulin. J Cell Sci 114:413–422

Jordan M, Wilson L (2004) Mary Ann Jordan, Leslie Wilson. Nat Rev Cancer 4:253–265

Kikkawa M et al (2001) Switch-based mechanism of kinesin motors. Nature 411:439–445

Kirschner M, Schulze E (1986) Morphogenesis and the control of microtubule dynamics in cells. J Cell Sci Suppl 5:293–310

Laskowski RA et al (1993) PROCHECK: a program to check the stereochemical quality of protein structures. J Appl Crystallogr 26:283–291

Li H et al (2002) Microtubule structure at 8 A resolution. Structure (Camb) 10:1317–1328

Lindahl E, Hess B, Van Der Spoel D (2001) GROMACS 3.0: a package for molecular simulation and trajectory analysis. J Mol Mod 7:306–317

Lowe J et al (2001) Refined structure of alpha beta-tubulin at 3.5 A resolution. J Mol Biol 313:1045–1057

Lu Q, Luduena R (1994) In vitro analysis of microtubule assembly of isotypically pure tubulin dimers. Intrinsic differences in the assembly properties of alpha beta II, alpha beta III, and alpha beta IV tubulin dimers in the absence of microtubule-associated proteins. J Biol Chem 269:2041–2047

Luduena R (1998) Multiple forms of tubulin: different gene products and covalent modifications. Int Rev Cytol 178:207–275

Mandelkow E, Mandelkow E (1992) Microtubule oscillations. Cell Motil Cytoskeleton 22:235–244

Margolis R, Wilson L (1981) Microtubule treadmills—possible molecular machinery. Nature 293:705–711

Melki R et al (1989) Cold depolymerization of microtubules to double rings: geometric stabilization of assemblies. Biochemistry 28:9143–9152

Minoura I, Muto E (2006) Dielectric measurements of individual microtubles using the electroorientation method. Biophys J 90:3739–3748

Mitchison T, Kirschner M (1984) Dynamic instability of microtubule growth. Nature 312:237–242

Nettles J et al (2004) The binding mode of epothilone A on alpha, beta-tubulin by electron crystallography. Science 305:866–869

Nogales E, Wolf S, Downing K (1998) Structure of the alpha beta tubulin dimer by electron crystallography. Nature 391:199–203

Oakley B et al (1990) Gamma-tubulin is a component of the spindle pole body that is essential for microtubule function in *Aspergillus nidulans*. Cell 61:1289–1301

Panda D et al (1994) Microtubule dynamics in vitro are regulated by the tubulin isotype composition. Proc Natl Acad Sci USA 91:11358–11362

Pichichero M, Avers C (1973) The evolution of cellular movement in eukaryotes: the role of microfilaments and microtubules. Subcell Biochem 2:97–105

Ravelli R et al (2004) Insight into tubulin regulation from a complex with colchicine and a stathmin-like domain. Nature 428:198–202

Roach MC et al (1998) Preparation of a monoclonal antibody specific for the class I isotype of beta-tubulin: the beta isotypes of tubulin differ in their cellular distributions within human tissues. Cell Motil Cytoskeleton 39:273–285

Sanchez R, Sali A (2000) Comparative protein structure modeling. Introduction and practical examples with modeller. Methods Mol Biol 143:97–129

Schlieper D et al (2005) Structure of bacterial tubulin BtubA/B: evidence for horizontal gene transfer. Proc Natl Acad Sci USA 102:9170–9175

Schoutens JE (2005) Dipole‘ dipole interactions in microtubules. J Biol Phys 31:35–55

Schuessler HA et al (2003) Surface plasmon resonance study of the actin-myosin sarcomeric complex and tubulin dimers. J Mod Optics 50:2381–2391

Sept D, Baker NA, Mccammon J (2003) The physical basis of microtubule structure and stability. Protein Sci 12:2257–2261

Stracke R et al (2002) Analysis of the migration behaviour of single microtubules in electric fields. Biochem Biophys Res Commun 293:602–609

van Gunsteren WF (1996) Biomolecular simulation: the GROMOS96 manual and user guide. Hochschulverlag AG an der ETH Zurich, Zurich

Walker R, Pryer NK, Salmon E (1991) Dilution of individual microtubules observed in real time in vitro: evidence that cap size is small and independent of elongation rate. J Cell Biol 114:73–81

Westermann S et al (2006) The Dam1 kinetochore ring complex moves processively on depolymerizing microtubule ends. Nature 440:565–569